Liquid Crystals
Publication details, including instructions for authors and subscription information:
http://www.informaworld.com/smpp/title~content=t713926090

Simulation studies of dipole correlation in the isotropic liquid phase

Melanie J. Cook[a]; Mark R. Wilson[a]
[a] Department of Chemistry, University of Durham, South Road, Durham DH1 3LE, UK,

Online publication date: 06 August 2010

To cite this Article Cook, Melanie J. and Wilson, Mark R.(2000) 'Simulation studies of dipole correlation in the isotropic liquid phase', Liquid Crystals, 27: 12, 1573 — 1583
To link to this Article: DOI: 10.1080/026782900750037149
URL: http://dx.doi.org/10.1080/026782900750037149

LIQUID CRYSTALS, 2000, VOL. 27, NO. 12, 1573–1583

Simulation studies of dipole correlation in the isotropic liquid phase

MELANIE J. COOK and MARK R. WILSON*

Department of Chemistry, University of Durham, South Road, Durham DH1 3LE, UK

(*Received 23 October 1999; in final form 1 March 2000; accepted 27 March 2000*)

The Kirkwood correlation factor g_1 determines the preference for local parallel or antiparallel dipole association in the isotropic phase. Calamitic mesogens with longitudinal dipole moments and Kirkwood factors greater than 1 have an enhanced effective dipole moment along the molecular long axis. This leads to higher values of $\Delta\varepsilon$ in the nematic phase. This paper describes state-of-the-art molecular dynamics simulations of two calamitic mesogens 4-(*trans*-4-*n*-pentylcyclohexyl)benzonitrile (PCH5) and 4-(*trans*-4-*n*-pentylcyclohexyl)chlorobenzene (PCH5-Cl) in the isotropic liquid phase using an all-atom force field and taking long range electrostatics into account using an Ewald summation. Using this methodology, PCH5 is seen to prefer antiparallel dipole alignment with a negative g_1 and PCH5-Cl is seen to prefer parallel dipole alignment with a positive g_1; this is in accordance with experimental dielectric measurements. Analysis of the molecular dynamics trajectories allows an assessment of why these molecules behave differently.

1. Introduction

The Kirkwood-Frohlich equation [1]

$$\frac{(\varepsilon - n^2)(2\varepsilon + n^2)}{\varepsilon(n^2 + 2)^2} = \frac{N\mu_{\text{eff}}^2}{9\varepsilon_0 k_B T} \tag{1}$$

is commonly used in dielectric studies of isotropic liquids. It allows a value for the mean square dipole moment μ_{eff}^2 to be determined from measurements of the electric permittivity ε (static dielectric constant) and the refractive index n for a molecular number density N. Local dipole–dipole interactions occur in most polar molecules and in these cases μ_{eff}^2 differs from the mean square dipole moment μ^2

$$\mu_{\text{eff}}^2 = g_1 \mu^2. \tag{2}$$

Here, g_1 is the Kirkwood correlation factor

$$g_1 = 1 + \frac{1}{N}\left\langle \sum_i^N \sum_{j \neq i}^N \cos\theta_{ij} \right\rangle \tag{3}$$

where θ_{ij} is the angle between the dipole vectors in molecules i and j and $\langle\ \rangle$ indicates an ensemble average.

Calamitic liquid crystal molecules with longitudinal dipole moments often exhibit a preferred antiparallel dipole-correlation leading to values of $g_1 < 1$ in the isotropic phase. This is undesirable in mesogens designed for twisted nematic displays. A tendency for antiparallel dipole association reduces the value of the effective dipole moment parallel to the molecular long axis in the nematic phase, reduces the dielectric anisotropy $\Delta\varepsilon = \varepsilon_\parallel - \varepsilon_\perp$, and raises the threshold voltage for electro-optic switching.

Small changes in molecular structure often give rise to significant changes in molecular properties in liquid crystals. For example, the two molecules 4-(*trans*-4-*n*-pentylcyclohexyl)benzonitrile (PCH5) and 4-(*trans*-4-*n*-pentylcyclohexyl)chlorobenzene (PCH5-Cl), shown in figure 1, vary only in the dipolar functional group attached to the phenyl ring. However, PCH5 exhibits a nematic phase with a clearing point at 328 K, but PCH5-Cl has a crystal to isotropic liquid transition at 305 K and a virtual nematic–isotropic transition at 277 K. The two materials also differ in their dipole correlation.

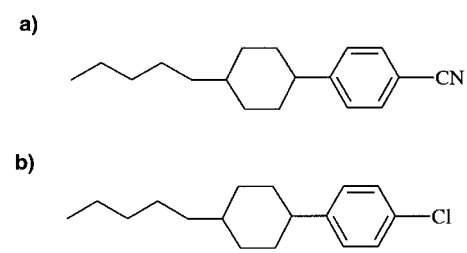

Figure 1. The molecular structures for the two molecules used in this study. (*a*) 4-(*trans*-4-*n*-pentylcyclohexyl)benzonitrile (PCH5), (*b*) 4-(*trans*-4-*n*-pentylcyclohexyl)chlorobenzene (PCH5-Cl).

*Author for correspondence; e-mail: Mark.Wilson@durham.ac.uk

Experiment shows that in the isotropic phase PCH5 prefers antiparallel dipole association ($g_1 = 0.88$, measured at 343 K) and PCH5-Cl favours parallel dipole association ($g_1 = 1.20$, measured at 309 K). The aim of the current paper is to use atomistic simulation methods [2, 3] to make reliable predictions for dipole correlation in these molecules and determine why they behave differently. We use state-of-the-art molecular dynamics techniques to simulate the isotropic phase for both systems, and we examine the important molecular configurations that are responsible for the differences in dipole correlation in the two mesogens.

The structure of this paper is as follows. The simulation model is described in detail in § 2.2, results for g_1 are presented in § 3 along with a detailed analysis of the antiparallel and parallel correlation between different groups in each molecule. Finally, in § 4, we make some general comments on the atomistic simulation of mesogens and the use of our method in designing molecules with large effective dipole moments.

2. Computational model

2.1. *Molecular force field*

The molecules PCH5 and PCH5-Cl work are represented as flexible entities composed of a series of atom-based potential energy functions

$$E_{\text{total}} = \sum_{\text{angle}} K_\theta(\theta - \theta_{\text{eq}})^2 + \sum_{\text{dihedral}} \left\{ \sum_{m=1}^{3} \frac{V_m}{2}[1 + \cos(m\phi - \delta_m)] \right\} + \sum_{i<j} \left(\frac{q_i \cdot q_j}{r_{ij}} + \frac{A_{ij}}{r_{ij}^{12}} - \frac{C_{ij}}{r_{ij}^{6}} \right) f_{ij} \quad (4)$$

where θ and θ_{eq} are the actual and equilibrium bond angles, ϕ and δ_m are dihedral and phase angles, and K_θ, V_m are force constants representing bond bending and torsional motion, respectively. The non-bonded energies between atoms i and j at a distance r_{ij} are represented by a Coulomb plus Lennard–Jones potential, where A_{ij} and C_{ij} can be expressed in terms of the well depth and collision parameters, ε_{ij} and σ_{ij}, respectively: $A_{ij} = 4\varepsilon_{ij}\sigma_{ij}^{12}$, $C_{ij} = 4\varepsilon_{ij}\sigma_{ij}^{6}$. ($f_{ij} = 0.5$ for 1,4 12:6 non-bonded terms, $f_{ij} = 0.125$ for 1,4 electrostatic terms and $f_{ij} = 1$ for all other non-bonded interactions.) In the current work we have used the OPLS-AA *all-atom force field* of Jorgensen and co-workers [4–6]. The non-bonded terms in this force field have been designed with the aim of predicting the correct densities and heats of vaporization for a series of small molecules. This is important for work of this type where errors in the predicted density will influence significantly the temperature of the clearing point/melting point of the molecule, and hence the calculated properties in the pretransitional region of the isotropic phase. The non-bonded parameters used are summarized in tables 1 and 2 and the numerous force field parameters for the internal molecular geometry are summarized in [4–6]. We note that the partial charges of table 1 are significantly higher than those calculated from Mullikan charge distributions obtained from standard basis set *ab initio* molecular orbital calculations. The latter are unable to represent properly the molecular quadrupole that arises from charge separations in the phenyl ring. We note that Yakovenko and co-workers [7–9] have recently simulated a united atom model of PCH5 with the aim of studying the properties of the isotropic and nematic phases. In this work however, we require a far more detailed model with a full treatment of the long range electrostatic interactions.

Table 1. Partial charges used for each atom type.

Atom (group)	Partial electronic charge/e^-
C(phenyl)	− 0.115
H(phenyl)	0.115
C(R_3CH)	− 0.060
C(R_2CH_2)	− 0.120
C(RCH_3)	− 0.180
H(RH,alkyl)	0.060
C(C−CN,phenyl)	0.395
C(CN)	0.035
N(CN)	− 0.430
C(C−Cl,phenyl)	0.191
Cl(C−Cl)[a]	− 0.191

[a] Calculated from bond dipole moment.

Table 2. 12:6 non-bonded parameters for PCH5 and PCH5-Cl.

Atoms (groups)	ε_{ij}/kJ mol^{-1}	σ_{ij}/Å
C=C	0.29288	3.550
C(phenyl)−H	0.19246	3.524
C(phenyl)−C	0.28451	3.525
C(phenyl)−CN	0.42677	3.599
C(phenyl)−N	0.45606	3.370
C(phenyl)−Cl	0.35146	3.976
$C(CH_2)$−$C(CH_2)$	0.27614	3.500
$C(CH_2)$−H	0.18410	2.958
$C(CH_2)$−C(N)	0.41422	3.574
$C(CH_2)$−N	0.44350	3.346
$C(CH_2)$−Cl	0.33974	3.948
H−H	0.12552	2.500
H−C(CN)	0.28033	3.021
H−Cl	0.23012	3.337
H−N	0.29706	2.828
C(CN)−C(CN)	0.62760	3.650
Cl−Cl	0.41840	4.454
C(CN)−N	0.66526	3.418
N−N	0.71128	3.200

2.2. *Molecular dynamics simulations*

For each system, an initial molecular configuration was generated from a *bcc* lattice in which 125 molecules were given a small random displacement from their lattice positions and randomly orientated inside a cuboidal simulation box at gas phase densities. Initially, the isothermal–isobaric algorithm of Berendsen was employed to relax the molecular configuration. We used a nominal pressure of 10^5 Pa until the desired volume of approximately 6.4×10^4 Å^3 had been achieved. Thereafter the system was equilibrated using a Nosé–Hoover thermostat and a Hoover barostat at a pressure of 1 atmosphere, employing relaxation times of 1 and 4 ps, respectively. The simulations retained cubic periodic boundary conditions throughout, employing the Verlet leap-frog algorithm with a time-step of 2 fs. The *long range* electrostatic interactions were handled by a Ewald sum with the convergence parameter α set at 0.48 Å^{-1} and 6 k-vectors were used for each of the directions (x, y, z) in the periodic box. A cut-off of 9 Å was used for the *short range* 12:6 interactions. All calculations used the DL_POLY_2.11 program [10].

Values of the system density ρ were monitored throughout the simulations along with g_1 values calculated from equation (3) and values of the orientational correlation factor

$$g_2 = 1 + \frac{1}{N}\left\langle \sum_i^N \sum_{j \neq i}^N P_2(\cos\theta_{ij}) \right\rangle$$
$$= 1 + \frac{1}{N}\left\langle \sum_i^N \sum_{j \neq i}^N \frac{3}{2}\cos^2\theta_{ij} - \frac{1}{2} \right\rangle. \qquad (5)$$

For both g_1 and g_2 we used the angles between the dipole vector (along the C–N and C–Cl bonds) to calculate θ_{ij}. Initial simulations of PCH5 were carried out in the pretransitional region of the isotropic phase at 343 K (table 3). Full equilibration of the system density required approximately 200 ps. Single particle properties (including g_1 and g_2) were seen to fluctuate rapidly during the early stages of the simulation when densities were low and molecular reorientation was rapid. After the equilibrated density was reached, a further period of 100 ps was allowed for these quantities to converge to their equilibrium values. Finally, results were calculated over a further simulation 600 ps production run. Further shorter simulations were performed at the higher temperature of 377 K to assess the temperature dependence of the results. Here, we allowed for 300 ps of equilibration time, starting from the end point of the lower temperature simulations and a further 200 ps production run to compute simulation data. For PCH5-Cl we also carried out initial simulations at 343 K. Here, the density required 200 ps to equilibrate, and a further 400 ps were allowed for the equilibration of g_1 and g_2. The production run was carried out over a further 300 ps. Finally, the temperature was dropped to 309 K and a further 300 ps was allowed for equilibration at this temperature. This was followed by a 300 ps production run.

3. Results and discussion

3.1. *Density, dipole and orientational correlation*

The computed values of the system density $\langle \rho \rangle$ for PCH5 and PCH5-Cl are given in table 3. $\langle \rho \rangle$ values are in excellent agreement with experiment for both systems (better than 1%) and are a good indication of the accuracy of the intermolecular force field used. Recent work by Jorgensen *et al.* [4] to design high accuracy force fields for small molecules has specifically used the system density to fit the non-bonded parameters in the force field. The density turns out to be quite sensitive to the intermolecular parameters and small changes in these lead to significant changes in the density. We have used the Jorgensen non-bonded parameters in the force field for this work, and it is encouraging that the same parameters that predict the correct density for small molecules seem to be directly transferable to mesogens. We also note the importance of correctly treating the long range part of the electrostatic interactions, because this can also have a significant influence on the system density.

In the isotropic liquid phase we expect dipolar and orientation correlation to be short range and to decay to zero within the simulation box. To check this we calculated the distance dependent correlation functions

$$g_l(r) = \langle P_l \cos(\theta_{ij}) \rangle_{\text{shell}}, \qquad l = 1, 2 \qquad (6)$$

Table 3. Box lengths, computed densities and order parameters from simulations of PCH5 and PCH5-Cl.

Molecule	Simulation T/K	$\langle$ Boxsize$\rangle$ /Å	$\langle \rho \rangle$ /kg m^{-3}	ρ(exp)/kg m^{-3}	$\langle S_2 \rangle$ (from λ_-)	$\langle S_2 \rangle$ (from λ_+)
PCH5	343	38.50	928.7 ± 3.6	926	0.05	0.15
PCH5	377	38.54	926.0 ± 4.5	—	0.03	0.19
PCH5-Cl	309	38.28	978.6 ± 3.7	986	− 0.05	0.08
PCH5-Cl	343	38.43	967.3 ± 3.6	—	0.00	0.19

where $\langle\ \rangle_{\text{shell}}$ indicates an ensemble average over molecules j in a spherical shell of width dr at a distance r between the centres of the dipolar groups of molecules i and j.

Graphs of $g_1(r)$ and $g_2(r)$ for PCH5 and PCH5-Cl are plotted in figures 2 and 3, respectively. For $g_1(r)$, positive values indicate a preferred parallel alignment of dipoles at a distance r and negative values indicate a preferred antiparallel alignment. The $g_1(r)$ graphs show a clear distinction between the behaviour of PCH5 and PCH5-Cl at small r. PCH5 exhibits a strong preference for antiparallel association with a pronounced trough in $g_1(r)$ for $r \approx 4.0$–5.5 Å and PCH5-Cl exhibits a preference for parallel association through a small peak in $g_1(r)$ for $r \approx 4.0$–5.0 Å at 309 K. For the higher temperature PCH5 simulation, the position of the trough sharpens somewhat, but the area under it drops significantly. The broad trough at 343 K is indicative of a series of preferred antiparallel configurations of varying energy (see § 3.2). At higher temperatures molecules have more energy and some of the higher energy antiparallel configurations become less favoured at 377 K. The peak in $g_1(r)$ for PCH5-Cl reduces considerably as the temperature is raised and further from the phase transition at 343 K the preference for parallel dipole association has almost disappeared.

Both $g_1(r)$ (in figure 2) and $g_2(r)$ (in figure 3) tend towards zero as r increases, but small fluctuations in order remain even at long distances. This is typical for simulations of relatively small systems. Short range orientational fluctuations are propagated across the system by the periodic boundary conditions and the average value of the system order parameter $S_2 = \langle P_2(\cos\theta)\rangle$ is therefore non-zero (usually $0.1 < S_2 < 0.2$). To check this we calculated $\langle S_2\rangle$ from the largest eigenvalue λ_+ obtained through the standard method of diagonalizing the ordering tensor

$$Q_{\alpha\beta} = \frac{1}{N}\sum_{j=1}^{N}\frac{3}{2}u_{j\alpha}U_{j\beta} - \frac{1}{2}\delta_{\alpha\beta}, \qquad \alpha, \beta = x, y, z. \quad (7)$$

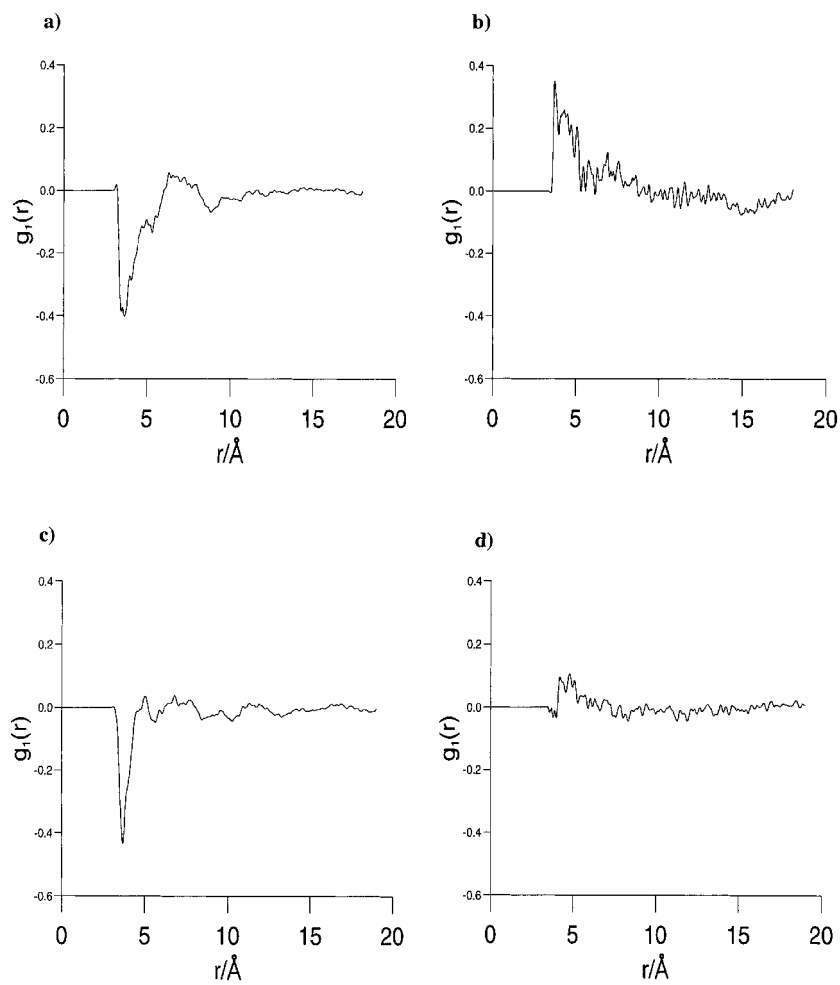

Figure 2. Pair correlation functions $g_1(r)$ for PCH5 and PCH5-Cl. (*a*) PCH5 at $T = 343$ K, (*b*) PCH5-Cl at $T = 309$ K, (*c*) PCH5 at $T = 377$ K, (*d*) PCH5-Cl at $T = 343$ K.

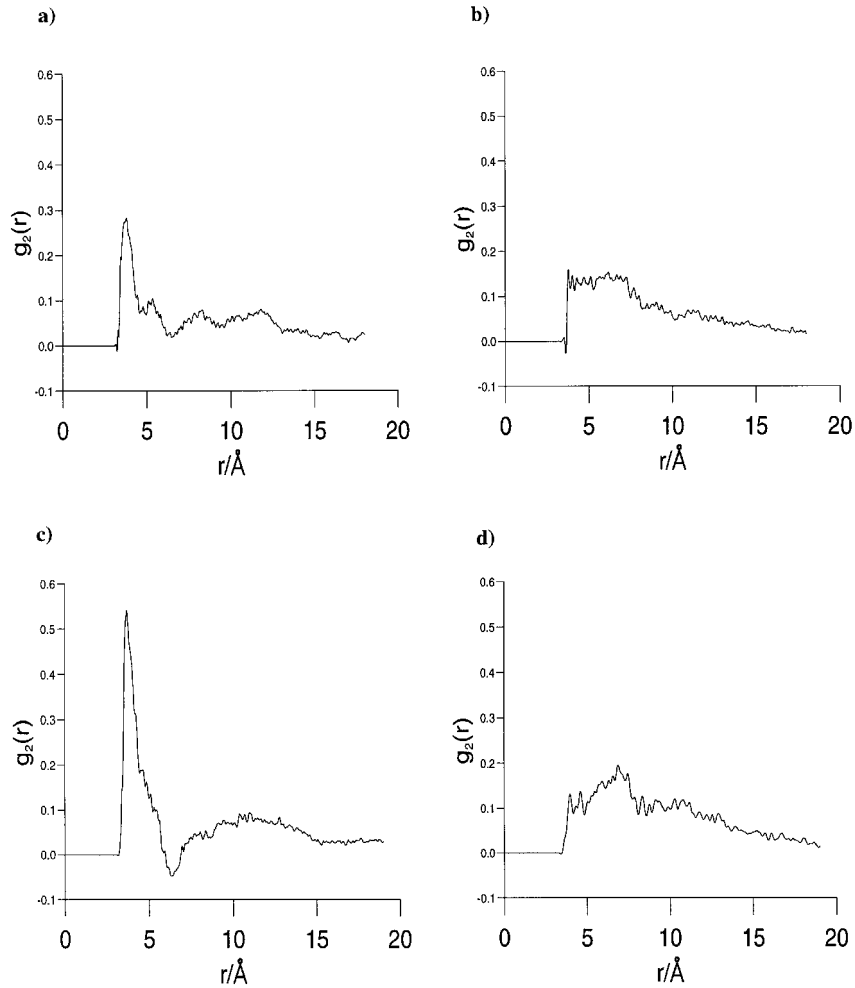

Figure 3. Pair correlation functions $g_2(r)$ for PCH5 and PCH5-Cl. (*a*) PCH5 at $T = 343$ K, (*b*) PCH5-Cl at $T = 309$ K, (*c*) PCH5 at $T = 377$ K, (*d*) PCH5-Cl at $T = 343$ K.

The vector $\mathbf{u}_j$ in equation (7) is defined as the molecular long axis obtained through diagonalization of the moment of inertia tensor [11]

$$I_{\alpha\beta} = \sum_i m_i(s_i^2 \delta_{\alpha\beta} - s_{i\alpha} s_{i\beta}) \tag{8}$$

where the atomic distance vectors $\mathbf{s}_i$ were measured relative to the molecular centre of mass. For relatively small systems, this standard approach to calculate $\langle S_2 \rangle$ often exaggerates the order in the system, because λ_+ is always greater than zero. An alternative (and often better) approach for the isotropic phase is to follow Eppenga and Frenkel [12] and to calculate S_2 from $-2 \times$ the middle eigenvalue λ_0 of the ordering tensor. The calculated order parameters for each simulation are given in table 3. The values are typical of those calculated in the pretransitional region of the isotropic phase for similar sized systems of single-site potentials (hard-spherocylinders and Gay–Berne fluids). Unexpectedly, in both systems the values of $\langle S_2 \rangle$ are slightly larger for the higher temperature system. This is simply an indication of the errors associated with simulations of relatively small systems such as this. Simulations of larger numbers of molecules using single-site potentials indicate that such *system size effects* diminish as the number of molecules increases above 1000.

The g_1 and g_2 values calculated from equations (3) and (5) are given in table 4. The g_1 results show reasonably good agreement with values obtained from experimental dielectric measurements and confirm the individual preferences for antiparallel (PCH5) and parallel (PCH5-Cl) dipole association in the isotropic phase. However, we emphasize the large error bars associated with these quantities and we note that the g_1 and (to a greater extent) g_2 values will be influenced by the fact

Table 4. Computed pair-wise correlation factors g_1 and g_2.

Molecule	T/K	g_1	g_2	g_1(exp)
PCH5	343	0.66 ± 0.04	3.63 ± 0.25	0.88
PCH5	377	0.95 ± 0.07	4.41 ± 0.26	—
PCH5-Cl	309	1.06 ± 0.02	4.81 ± 0.05	1.20
PCH5-Cl	343	1.22 ± 0.02	4.08 ± 0.17	—

that the distance-dependent correlation functions do not fully decay to zero within the simulation box. We therefore expect the calculated g_1 and (in particular) g_2 values to be dependent on the system size. More reliable values can only be achieved by simulations with a larger number of molecules. The values obtained for g_2 for both materials are similar to those seen in simulation studies of ($L/D = 3$) hard ellipsoids in the pretransitional region [13]. Values of g_2 usually increase as the isotropic–nematic transition is approached, and can reach values of $g_2 \approx 100$ at temperatures very close to the isotropic–nematic phase transition [14]. We would therefore expect the lower temperature simulations to exhibit slightly higher values of g_2. This is seen for PCH5-Cl, but not for PCH5. We note however that our error bars for g_2 are rather large. In addition, local fluctuations in orientational order are exaggerated in importance within a relatively small simulation box and our g_2 results reflect these *system size induced* errors.

3.2. *Correlation between molecular groups*

It is interesting to consider which interactions are responsible for the difference in dipole correlation of the two molecules. In the liquid phase we expect the molecules to be continually moving with respect to each other. However, we expect the local structure of the fluid to be influenced by configurations where molecules experience strong local interactions. Such interactions momentarily cause them to stay in those configurations longer than they would do in the absence of strong group–group interactions. A detailed insight into the local molecular alignment of the molecules is achieved by defining a two-dimensional distribution function $g(r, \pm|z|)$ as indicated in figure 4

$$\text{for} \quad \mathbf{r}_i \ \mathbf{r}_j \geqslant 0,$$
$$g(r, +|z|) = \frac{V}{N^2}\left\langle \sum_i \sum_{j \neq i} \delta(\mathbf{r} - \mathbf{r}_{ij})\delta(z - |z_{ij}|) \right\rangle$$
$$\text{for} \quad \mathbf{r}_i \ \mathbf{r}_j \leqslant 0, \tag{9}$$
$$g(r, -|z|) = \frac{V}{N^2}\left\langle \sum_i \sum_{j \neq i} \delta(\mathbf{r} - \mathbf{r}_{ij})\delta(z + |z_{ij}|) \right\rangle.$$

Here, $\mathbf{r}_i, \mathbf{r}_j$ are the axis vectors of the groups used in each molecule, $r_{ij} = |\mathbf{r}_i - \mathbf{r}_j|$ is the distance of separation between the centres of the two groups and the distances $|z_{ij}|$ are the absolute values of the projection of $\mathbf{r}_{ij}$ onto the axis vector of each molecular group (as shown in figure 4). In equation (9) we actually compile two separate functions $g(r, \pm|z|)$ depending on the angles between the axis vectors of molecules i and j. However, we represent them on a single plot by using positive values ($+|z|$) to represent parallel alignment (at $\mathbf{r}_i \ \mathbf{r}_j \geqslant 0$) and negative values ($-|z|$) to represent anti-parallel alignment (at $\mathbf{r}_i \ \mathbf{r}_j \leqslant 0$). In compiling $g(r, \pm|z|)$ histograms we consider the positional correlation between phenyl, cyclohexyl, and dipolar groups (C−CN, C−Cl). This generates the six two dimensional distribution functions shown in figures 5 (for PCH5) and 6 (PCH5-Cl).

It is clear from figures 5 and 6 that the correlation of individual groups is different in the two systems. Detailed analysis of the distribution functions concludes that in both cases a number of parallel and antiparallel dipole dimers exist. To see this we catalogue the individual peaks in $g(r, \pm|z|)$ in tables 5 and 6 and then assign

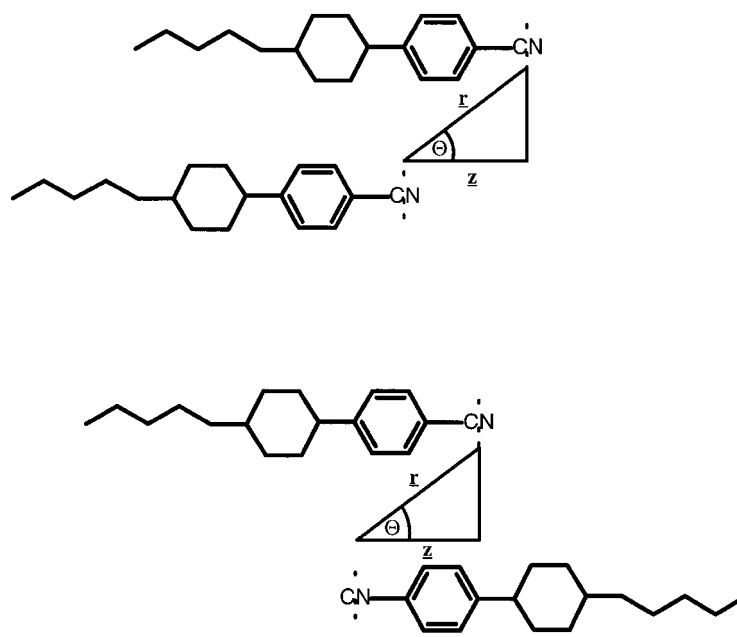

Figure 4. Schematic diagram showing the definition of the inter-group distances r and z for the two-dimensional pair correlation functions $g(r, \pm|z|)$.

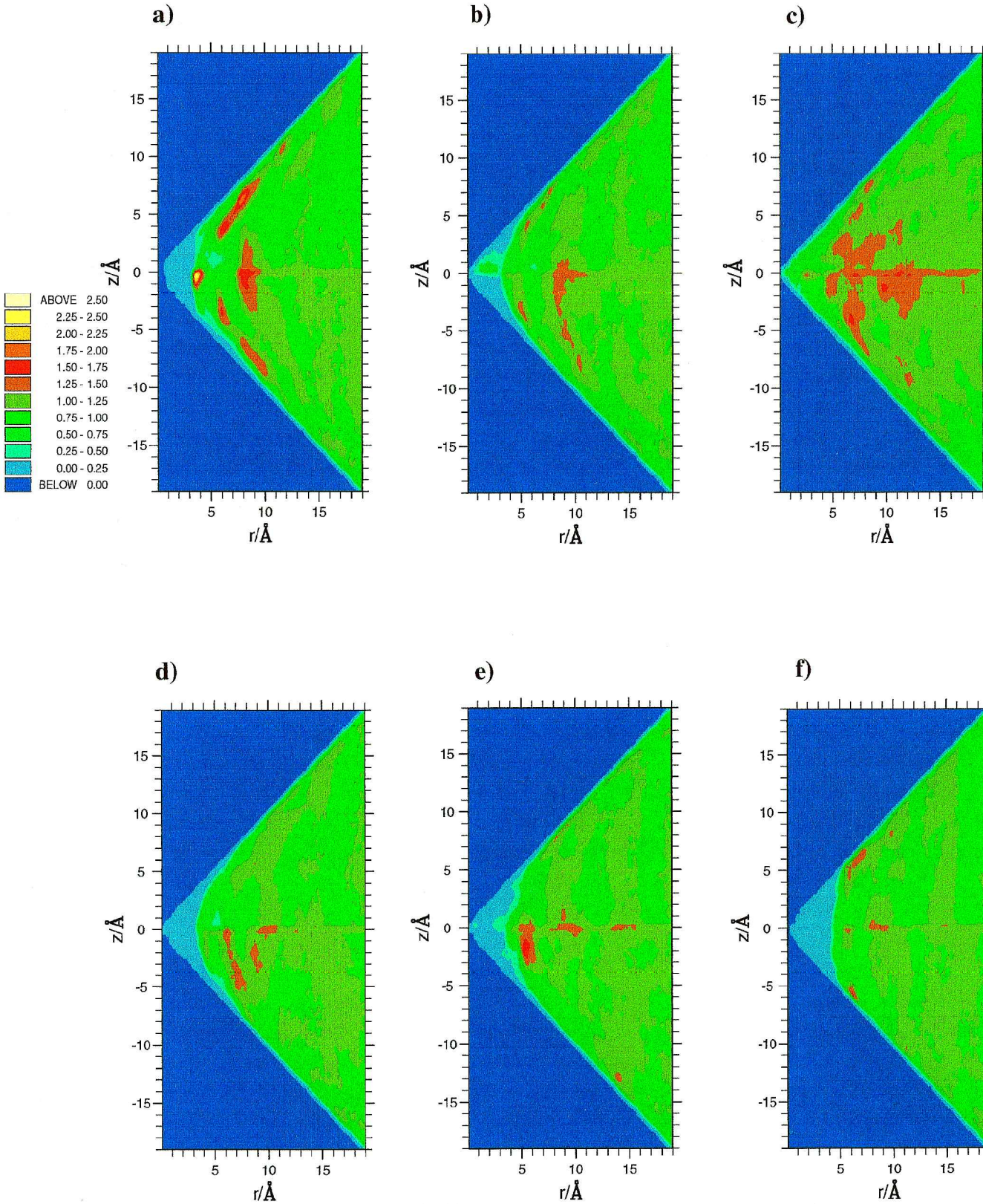

Figure 5. Two-dimensional correlation functions $g(r, \pm|z|)$ for individual groups in the molecule PCH5 at $T = 343$ K. (*a*) C−CN—C−CN, (*b*) C−CN—phenyl, (*c*) C−CN—cyclohexyl, (*d*) phenyl—phenyl, (*e*) phenyl—cyclohexyl, (*f*) cyclohexyl—cyclohexyl.

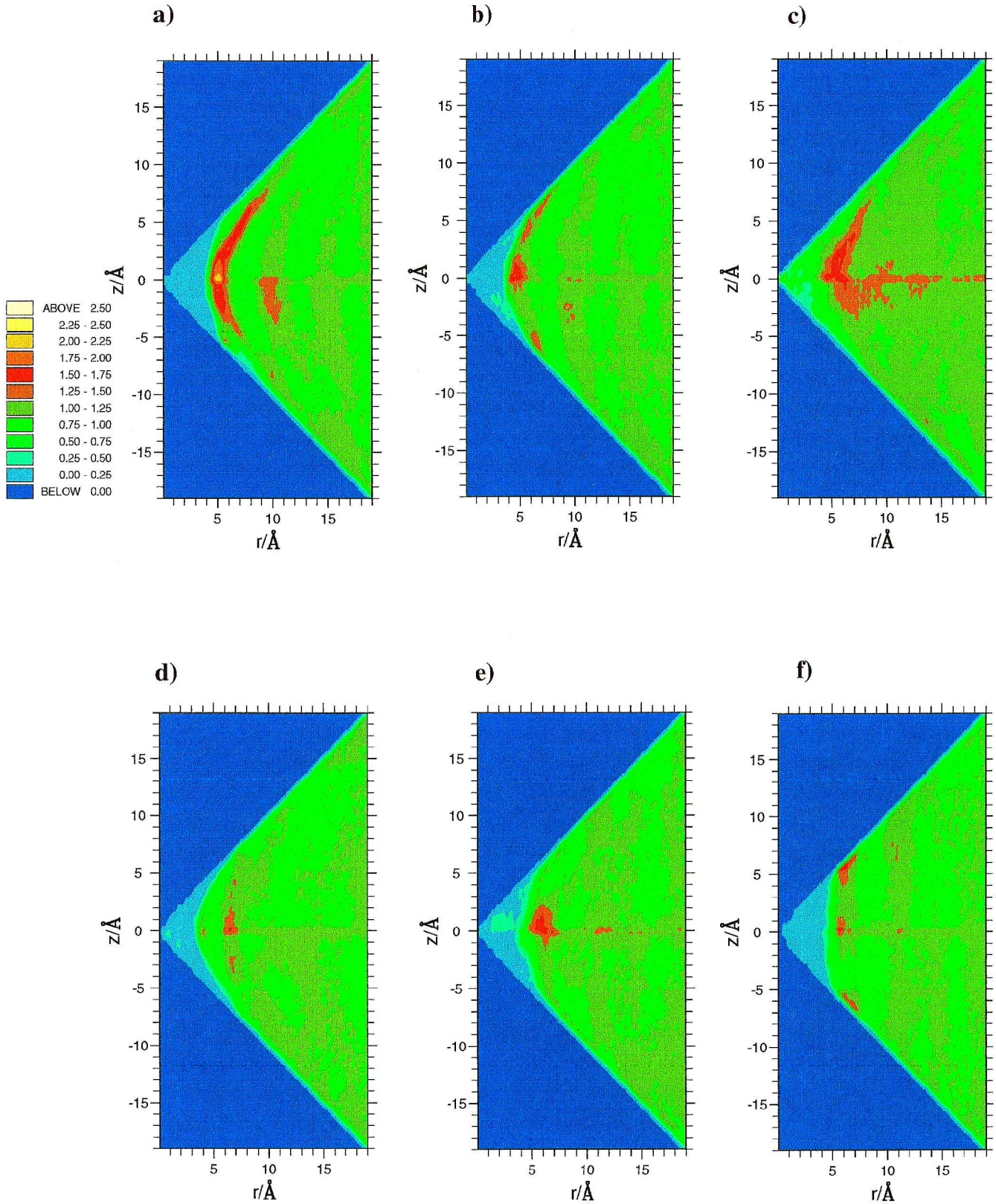

Figure 6. Two-dimensional correlation functions $g(r, \pm|z|)$ for individual groups in molecule PCH5-Cl at $T = 309$ K. (*a*) C–Cl—C–Cl, (*b*) C–Cl—phenyl, (*c*) C–Cl—cyclohexyl, (*d*) phenyl—phenyl, (*e*) phenyl—cyclohexyl, (*f*) cyclohexyl—cyclohexyl.

Table 5. Approximate positions of the main peaks in the two-dimensional translational correlation function $g(r, \pm|z|)$ for PCH5 at 343 K. Positive values of z indicate parallel association and negative values of z indicate anti-parallel association. Column four indicates the pair configuration(s) from figure 7 which are responsible for each peak ('secondary' indicates a peak that arises from next nearest neighbour interactions).

Group interactions	r/Å	z/Å	Configurations
C−CN—C−CN	4	0	A (strong correlation)
	8	0	A (strong, secondary)
	6	−4	G
	9	−8	E
	6	4	B
	8	6–7	C
C−CN—phenyl	9–10	0	G
	5	−3	F
	9	−5	F,E
	11	−8	E
C−CN—ring	7	0	C,F
	11	0	C (secondary)
	9	−2	G
	6	−4	E
phenyl—phenyl	6	0–−2	F
	7	−5	E
	9	−3	G
	11	0	F (secondary)
phenyl—cyclohexyl	6	0–−2	E
	9	0	E (secondary)
cyclohexyl—cyclohexyl	6	0	A,D
	9	0	A,D (secondary)
	6	−6	F
	7	6	C

Table 6. Approximate positions of the main peaks in the two-dimensional translational correlation function $g(r, \pm|z|)$ for PCH5-Cl at 309 K. Positive values of z indicate parallel association and negative values of z indicate anti-parallel association. Column four indicates the pair configuration(s) from figure 7 which are responsible for each peak ('secondary' indicates a peak that arises from next nearest neighbour interactions).

Group interactions	r/Å	z/Å	Configurations
C−Cl—C−Cl	5	0	A (strong)
	7	5	B (strong)
C−Cl—phenyl	5	1	A
	6	4	B,C
	7	6	C
	7	−6	F
C−Cl—ring	6	0–3	A,B
phenyl—phenyl	7	0–1	A
phenyl—cyclohexyl	6	0–1	B
	11	0	A (secondary)
cyclohexyl—cyclohexyl	6	0–1	A
	6	5	B

these peaks to specific molecular pair configurations. The main pair configurations that we expect to see are sketched in figure 7 and the assignment of pair configurations to specific peaks in $g(r, \pm|z|)$ is carried out in column four of tables 5 and 6.

Figures 5 and 6 show that the pair configurations that are energetically favoured change between PCH5 and PCH5-Cl. In PCH5 the most favoured pair configurations are G, E and A. In PCH5-Cl these change to A and B. The regions of high probability density for PCH5 result mainly from strong dipolar interactions involving the cyano groups and the phenyl rings. Such interactions favour anti-parallel arrangements of dipoles. However, PCH5-Cl has a much weaker dipole, and consequently dipolar interactions are less important relative to the favoured van der Waals interactions between the phenyl and cyclohexyl rings. We also note that the smaller dipole in PCH5-Cl means that interconversion between configurations such as A and B occurs far more easily than in PCH5. This is shown by the broad arc of probability density between $r = 5$, $z = 0$ and $r = 7$, $z = 5$ seen in the plot of $g(r, \pm|z|)$ for the C−Cl—C−Cl interactions, figure 6 (*a*).

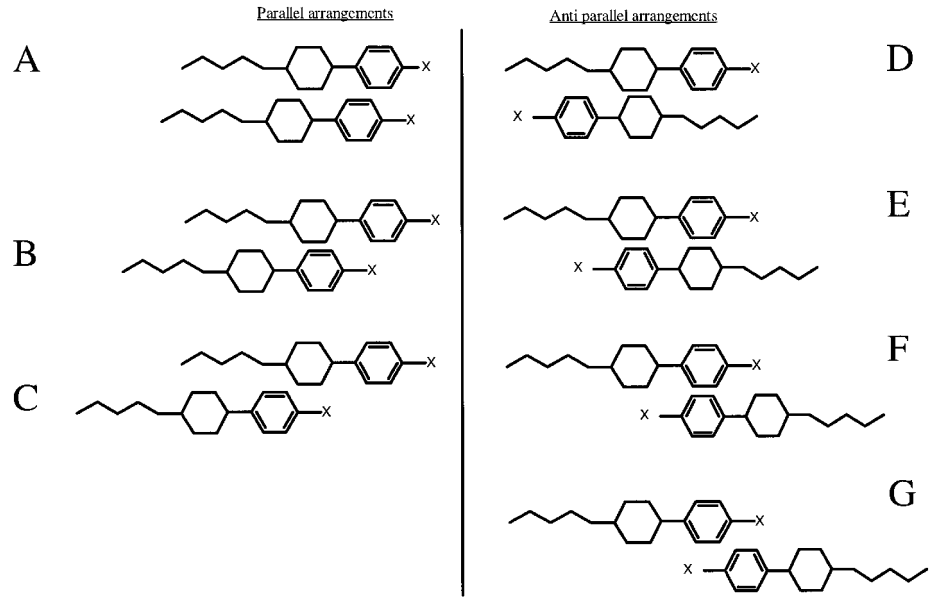

Figure 7. Schematic diagram showing favoured molecular pair configurations.

Our results are in agreement with experimental dielectric measurements for liquid crystal molecules in solutions in isotropic solvents [15, 16] which have also indicated the presence of parallel and antiparallel dipole dimers. The latter can be interpreted in terms of the Dunmur/Toriyama model for molecular association [15] which considers an equilibrium between parallel and antiparallel dipole species. We stress however that the Dunmur/Toriyama pair-wise association model is too simple to translate directly to the liquid phase. Here we find several preferred configurations for both parallel and antiparallel association, and this would translate to several equilibrium constants of different magnitude within the Dunmur/Toriyama model. In an early simulation study of liquid crystal systems [17], Wilson and Dunmur considered the interactions of pairs of PCH5 molecules in the gas phase and also reported a preference for antiparallel dipole association. We note however that the preferred liquid state dimers are rather different in structure to those predicted for the gas phase (figure 4 of [17]). The gas phase calculations indicated a preference for configuration D. This is not altogether surprising because this configuration allows for the strongest van der Waals attractions between a molecular pair. Maximizing van der Waals interactions between a molecular pair is less important in the liquid phase (or in a liquid crystal phase), because any pair of molecules is surrounded by a 'swarm' of neighbours with which it interacts.

The $g(r, \pm|z|)$ analysis illustrates the large effects that small changes in molecular structure can produce in terms of intermolecular interactions. It also points to the way in which careful molecular design can preferentially select favourable molecular interactions within liquid crystals in order to produce the desired effect in terms of molecular ordering. In the case of strongly dipolar molecules, dipole interactions usually favour antiparallel dipole alignment. However, it is believed that appropriate arrangements of functional groups within a molecule can combat this trend generating preferred parallel dipole association and increasing μ_{eff}^2 in the bulk phase. The $g(r, \pm|z|)$ analysis (above) provides a useful way to study the effects of individual functional groups via simulation. In the future these types of calculations may prove extremely valuable in terms of molecular engineering applications.

4. Conclusions

The calculations presented in this work represent the most accurate all-atom study of mesogenic molecules published to date. We are able to model successfully the different dipole-correlation behaviour of PCH5 and PCH5-Cl. This is best seen through the distance-dependent correlation functions $g_1(r)$ that show preferred antiparallel association for PCH5 and preferred parallel association for PCH5-C at short distances. We also determine g_1 values that are in qualitative agreement with experimental data and obtain excellent agreement between experimental and computed densities for both systems.

Extensive analysis of equilibrium MD trajectories has allowed us to determine which groups influence molecular association in the isotropic phase. We note that the picture of dipole correlation in the bulk is a complicated one. In the case of both molecules, several parallel and antiparallel dipole dimers can be detected, and it is the subtle differences in preference for individual molecular pair configurations that give rise to the different values of g_1.

Our calculations show that it is now possible to use atomistic simulation to predict bulk phase properties for mesogenic systems. Although these calculations are preliminary (in the sense that we have only studied two systems here), the results are encouraging and provide motivation for using techniques such as this in molecular engineering applications: to determine molecular properties prior to synthesis. In the case of g_1 calculations it should be possible in the near future for molecular simulation to determine which of a series of similar structures will give rise to the largest effective dipole moment in the condensed state. This is something which can currently only be hypothesized with the aid of considerable chemical intuition.

Finally, we note the importance of modelling intermolecular interactions as accurately as possible in order to account for the drastic changes in mesogen behaviour that result from small changes in molecular structure. Proper handling of long range forces is essential, resulting in a heavy computational load arising from an all-atom Ewald sum. The calculations described here required the equivalent of 800 CPU hours on state-of-the-art processors. However, we expect rapid advances in computer speed greatly to increase the accessibility of such calculations within the next few years.

The authors wish to thank the University of Durham IT service for providing computer time on its parallel Silicon Graphics system, and the UK EPSRC for providing computer time on a Cray T3E. M.J.C. wishes to thank the EPSRC and Merck UK Ltd for providing a research studentship (1997–2000), and Merck UK Ltd (Southampton) for the gift of a DEC 433 a.u. workstation. The authors wish to thank Dr M. Bremer and Dr M. Heckmeier (Merck KGaA, Darmstadt) for valuable discussions and for supplying experimental data for PCH5 and PCH5-Cl.

References

[1] Dunmur, D. A., and Toriyama, K., 1998, in *Handbook in Liquid Crystal*, Vol. 1, edited by D. Demus, J. Goodby, G. W. Gray, H.-W. Spiess, and V. Vill (Weinheim: Wiley-VCH), Chap. VII.4.

[2] Wilson, M. R., 1981, in *Handbook of Liquid Crystals*, Vol. 1, edited by D. Demus, J. Goodby, G. W. Gray, H.-W. Spiess, and V. Vill (Weinheim: Wiley-VCH), Chap. III.3.

[3] Wilson, M. R., 1999, in *Structure and Bonding: Liquid Crystals*, edited by M. Mingos (Springer-Verlag, Heidelberg), p. 41.

[4] Jorgensen, W. L., Maxwell, D. S., and Tirado-Rives, J., 1996, *J. Am. chem. Soc.*, **118,** 11 225.

[5] Jorgensen, W. L., Maxwell, D. S., and Tirado-Rives, J., 1996, *J. Am. chem. Soc.*, **118,** 11 225 (support material).

[6] Jorgensen, W. L., and Nguyen, T. B., 1993, *J. comput. Chem.*, **14,** 195.

[7] Yakovenko, S. Y., Muravski, A. A., Kromer, G., and Geiger, A., 1995, *Mol. Phys.*, **86,** 1099.

[8] Yakovenko, S. Y., Kromer, G., and Geiger, A., 1996, *Mol. Phys.*, **275,** 91.

[9] Yakovenko, S. Y., Muravski, A. A., Eikelschulte, F., and Geiger, A., 1998, *Liq. Cryst.*, **24,** 657.

[10] Smith, W., and Forester, T., 1996: DL_POLY is a package of molecular simulation routines; copyright The Council for the Central Laboratory of the Research Councils, Daresbury Laboratory at Daresbury, Nr. Warrington.

[11] Wilson, M. R., and Allen, M. P., 1992, *Liq. Cryst.*, **12,** 157.

[12] Eppenga, R., and Frenkel, D., 1984, *Mol. Phys.*, **52,** 1303.

[13] Veerman, J. A. C., and Frenkel, D., 1990, *Phys. Rev. A*, **41,** 3245.

[14] Wilson, M. R., 1988, PhD thesis, University of Sheffield, UK.

[15] Toriyama, K., and Dunmur, D. A., 1986, *Mol. Cryst. liq. Cryst.*, **139,** 123.

[16] Dunmur, D. A., and Toriyama, K., 1986, *Liq. Cryst.*, **1,** 169.

[17] Wilson, M. R., and Dunmur, D. A., 1989, *Liq. Cryst.*, **5,** 987.